

# Pessimistic Off-Policy Multi-Objective Optimization

Shima Alizadeh  
AWS AI Labs

Aniruddha Bhargava  
Amazon

Karthick Gopalswamy  
AWS AI Labs

Lalit Jain  
Amazon Visiting Scholar

Branislav Kveton  
AWS AI Labs

Ge Liu  
AWS AI Labs

## Abstract

Multi-objective optimization is a type of decision making problems where multiple conflicting objectives are optimized. We study offline optimization of multi-objective policies from data collected by an existing policy. We propose a pessimistic estimator for the multi-objective policy values that can be easily plugged into existing formulas for hypervolume computation and optimized. The estimator is based on inverse propensity scores (IPS), and improves upon a naive IPS estimator in both theory and experiments. Our analysis is general, and applies beyond our IPS estimators and methods for optimizing them. The pessimistic estimator can be optimized by policy gradients and performs well in all of our experiments.

## 1 Introduction

*Multi-objective optimization (MOO)* is an area of decision making where multiple conflicting objectives are optimized (Keeney and Raiffa, 1993; Emmerich and Deutz, 2018). Many real-world problems have multiple objectives, including in economics (Ponsich et al., 2013), engineering (Marler and Arora, 2004), product design and manufacturing (Wang et al., 2011), and logistics (Xifeng et al., 2013). Therefore, MOO has been applied widely and successfully. A typical setting is of a system designer that tries to trade off multiple objectives subject to their preferences. As an example, when designing a product, the form factor, cost, and failure rate must be carefully balanced.

MOO has been usually studied under the assumption that the objective function is known, with a focus on optimizing it. When it is not known, the problem of learning to optimize it online can be formulated as a *contextual bandit* (Li et al., 2010; Chu et al., 2011), where the goal is to learn a *policy* that takes the most rewarding *action* in each *context*. In many applications, policies cannot be learned online by bandit algorithms because exploration can significantly impact user experience. However, offline data collected by a previously deployed policy are often available. Offline, or *off-policy*, optimization using such logged data is a practical way of learning policies without costly online interactions (Dudik et al., 2014; Swaminathan and Joachims, 2015a). In this work, we study offline optimization of multi-objective policies from logged data.

One motivating example for our work is the design of a movie recommendation policy at a movie streaming company. As a first step, a policy could be learned offline to maximize the click-through rate (CTR). After it is deployed online, the policy recommends too many recent movies, which was not intended. To avoid this bias, a recent movie penalty is added to the objective and a new policy is learned offline. After it is deployed online, the policy recommends mostly classic movies, which was again not intended. Hence it needs to be redesigned again. A company typically goes through many iterations like this until a policy with a good balance between recency, popularity, and relevance is learned. We propose an offline framework for policy optimization that avoids this.

We study off-policy MOO from logged data and make the following contributions. First, we formalize offline optimization of multi-objective policies as hypervolume maximization. Second, we propose a pessimistic IPS estimator for the values of multi-objective policies that can be easily plugged into existing formulas for hypervolume computation. Third, we analyze the error of the estimator when used in optimization, and show its benefits over a naive IPS estimator. Our

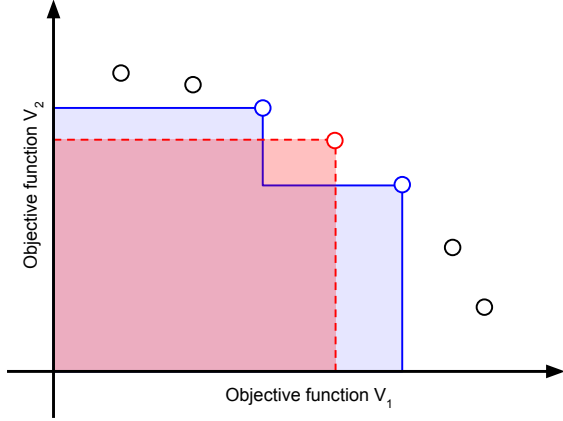


Figure 1: Each point is a value function  $V(\pi)$  for one policy  $\pi \in \Pi$ . The red rectangle is the optimal hyper-volume for  $K = 1$ . The union of the blue rectangles is the optimal hypervolume for  $K = 2$ .

analysis is general, and applies beyond our IPS estimators (Section 3) and methods for optimizing them (Section 5). Finally, we show the benefit of pessimistic optimization empirically on all major multi-objective benchmarks: ZDT (Zitzler et al., 2000), DTLZ (Deb et al., 2005), and WFG (Huband et al., 2005).

## 2 Setting

We formally introduce the problem of policy optimization with a single objective in Section 2.1 and generalize it to multiple objectives in Section 2.2.

### 2.1 Single-Objective Policy Optimization

We start with introducing our notation. Random variables are capitalized, except for Greek letters like  $\theta$ . For any positive integer  $n$ , we define  $[n] = \{1, \dots, n\}$ . The indicator function is  $\mathbb{1}\{\cdot\}$ . The  $i$ -th entry of vector  $v$  is denoted by  $v_i$ . If the vector is already indexed, such as  $v_j$ , we write  $v_{j,i}$ .

In the classic contextual bandit (Li et al., 2010), the agent observes a *context*  $x \in \mathcal{X}$ , where  $\mathcal{X}$  is a *context set*; takes an *action*  $a \in \mathcal{A}$ , where  $\mathcal{A}$  is an *action set*; and observes a *stochastic reward*  $Y \sim P(\cdot | x, a)$ , where  $P(\cdot | x, a)$  is the *reward distribution* of action  $a$  in context  $x$ . We denote the mean reward of action  $a$  in context  $x$  by  $r(x, a) = \mathbb{E}_{Y \sim P(\cdot | x, a)}[Y]$ . A *policy*  $\pi$  maps actions to contexts, and we denote by  $\pi(a | x)$  the probability of taking action  $a$  in context  $x$ .

Let  $(x_t)_{t=1}^n$  be a sequence of  $n$  contexts. The *expected*

value of policy  $\pi$  in contexts  $(x_t)_{t=1}^n$  is

$$V(\pi) = \frac{1}{n} \sum_{t=1}^n \sum_{a \in \mathcal{A}} \pi(a | x_t) r(x_t, a). \quad (1)$$

The optimal policy maximizes the expected value,

$$\pi_* = \arg \max_{\pi \in \Pi} V(\pi), \quad (2)$$

where  $\Pi$  is a class of optimized policies. If the policy class is sufficiently expressive,  $\pi_*$  could take the action with the highest mean reward in each context.

### 2.2 Multi-Objective Policy Optimization

Now we extend the setting in Section 2.1 to multiple objectives. The main difference is that the stochastic reward  $Y \sim P(\cdot | x, a)$  and its mean  $r(x, a)$  are vectors of length  $m$ , where  $m$  is the *number of objectives*. We denote by  $Y_i$  and  $r_i(x, a)$  the corresponding rewards in objective  $i \in [m]$ . The expected value of policy  $\pi$ ,  $V(\pi)$  in (1), is also an  $m$ -dimensional vector; and we denote by  $V_i(\pi)$  the value in objective  $i$ . We refer to  $V(\pi)$  as a *value function* since it maps policies to their values in multiple objectives. To simplify exposition, we assume that the stochastic rewards are bounded in  $[0, 1]^m$ . Thus  $r(x, a) \in [0, 1]^m$  and  $V(\pi) \in [0, 1]^m$ .

Our motivating movie recommendation problem can be formulated in our setting as follows. The context set  $\mathcal{X}$  is the set of all users and the action set  $\mathcal{A}$  is the set of all movies that can be recommended. The user in interaction  $t$ ,  $x_t \in \mathcal{X}$ , is recommended movie  $a \in \mathcal{A}$  with probability  $\pi(a | x_t)$ . The mean reward could have two components, the click probability  $r_1(x_t, a)$  and the purchase probability  $r_2(x_t, a)$ .

The main challenge in extending the optimization in (2) to multiple objectives is that no policy may dominate others in all objectives. To address this problem, we adopt a standard approach in *a-posteriori* MOO (Miettinen, 1998): we cover the Pareto front of  $V$  with diverse solutions  $\pi \in \Pi$ . Popular approaches for diversity maximization include random scalarization (Murata and Ishibuchi, 1995), Pareto dominance (Deb et al., 2002), and hypervolume maximization (Emmerich et al., 2005). We adopt the last approach. In our movie recommendation problem, the diverse set of policies would be learned and presented to a human decision maker, which would then select a policy that best fits their preferences.

We measure the diversity of policies by their *hypervolume indicator*, a popular metric in multi-objective optimization (Emmerich et al., 2005). The *hypervol-*

ume indicator of policies  $S \subseteq \Pi$  is defined as

$$\begin{aligned} \text{vol}(S, V) &= \int_{y \in [0,1]^m} \mathbb{1} \left\{ \bigvee_{\pi \in S} \{y \leq V(\pi)\} \right\} dy \quad (3) \\ &= \bigcup_{\pi \in S} \bigtimes_{i=1}^m [0, V_i(\pi)], \end{aligned}$$

where the inequality  $y \leq V(\pi)$  is applied entry-wise. The first definition says that it is the fraction of points  $y \in [0,1]^m$  such that  $y \leq V(\pi)$  holds for at least one  $\pi \in S$ . The second definition says that it is the hypervolume of a union of hyperrectangles corresponding to policies  $\pi \in S$ . To simplify terminology, we refer to (3) as the *hypervolume*.

Our goal is to identify  $\hat{S} \subseteq \Pi$  such that  $|\hat{S}| \leq K$  and  $\text{vol}(\hat{S}, V) \approx \text{vol}(\Pi, V)$ . Roughly speaking,  $\hat{S}$  should be as diverse as  $\Pi$ , as measured by covering a similar space. Thus a natural generalization of (2) is the set of  $K$  policies that maximizes the hypervolume,

$$S_* = \arg \max_{S \subseteq \Pi: |S|=K} \text{vol}(S, V). \quad (4)$$

We note that (4) reduces to (2) when the number of objectives is  $m = 1$ . We illustrate solutions to (4) for  $K \in \{1, 2\}$  in Figure 1.

In this work, we study a setting where the value function  $V$ , an input to  $\text{vol}(S, V)$ , is estimated from logged data. We give estimators of  $V$  in Section 3 and then analyze them in Section 4. We discuss algorithms for solving (4) using the estimators in Section 5.

### 3 Off-Policy Multi-Objective Estimation

The value function  $V$  is unknown but we can estimate it from data collected by another policy. We formalize this problem as follows. Let  $(x_t)_{t=1}^n$  be the same sequence of contexts as in (1) and  $\pi_0$  be a data *logging policy*  $\pi_0$ , which takes action  $A_t \sim \pi_0(\cdot | x_t)$  in interaction  $t \in [n]$ . Let  $Y_t = (Y_{t,i})_{i \in [m]}$  be the corresponding reward, generated as  $Y_t \sim P(\cdot | x_t, A_t)$ . The rewards are *stochastic* and sampled independently, with means  $\mathbb{E}[Y_{t,i} | x_t, A_t] = r_i(x_t, A_t)$  and  $\sigma^2$ -sub-Gaussian noise. The result of this process is a *logged dataset* of size  $n$ ,  $\mathcal{D} = \{(x_t, A_t, Y_t)\}_{t \in [n]}$ , which we use to estimate  $V$ .

The rest of this section is organized as follows. We present an inverse propensity score estimator of the value function  $V$  in Section 3.1. Our main contribution is its pessimistic variant in Section 3.2. We focus on these estimators because they can be easily combined with differentiable policies (Swaminathan and Joachims, 2015a). We discuss other possible choices in Appendix C. We design estimators separately for each

objective, which allows them to be plugged into existing hypervolume estimators. For instance, if  $\hat{V}_i(\pi)$  is an estimate of  $V_i(\pi)$ , we only need to replace  $V_i(\pi)$  in (3) to obtain hypervolume under that estimate. While the per-objective design appeared before in Wang et al. (2022), we are the first to incorporate pessimism and confidence intervals.

#### 3.1 IPS Estimator

One approach to off-policy optimization is to optimize the mean estimate  $\hat{V}$  of  $V$ . The advantage is that the uncertainty of  $\hat{V}$  does not have to be modeled. The most popular approach for estimating the mean value of a policy are *inverse propensity scores (IPS)* (Horvitz and Thompson, 1952). Generally, the value of policy  $\pi$  in objective  $i$  can be estimated using a *clipped IPS estimator* (Ionides, 2008; Strehl et al., 2010) as

$$\hat{V}_i(\pi, M) = \frac{1}{n} \sum_{t=1}^n \min \left\{ \frac{\pi(A_t | x_t)}{\pi_0(A_t | x_t)}, M \right\} Y_{t,i}, \quad (5)$$

where  $M \geq 0$  is a clipping parameter to control bias. The higher the value of  $M$ , the lower the bias and the higher the variance. When  $M = \infty$ , the estimator is unbiased but may suffer from a high variance. When  $M = 0$ , the estimator returns 0 for any policy  $\pi$ . We define the *IPS estimator* as  $\hat{V}_i(\pi) = \hat{V}_i(\pi, \infty)$ .

#### 3.2 Pessimistic IPS Estimator

Another approach to off-policy optimization is based on pessimism (Swaminathan and Joachims, 2015a; Jin et al., 2021; Hong et al., 2023), where a *lower confidence bound (LCB)* is optimized. The LCB can be derived using a high-probability confidence interval, which we derive below.

**Lemma 1.** Let  $c_i(\pi) = \beta \sigma M_\pi / n$  for  $\beta > 0$  and

$$M_\pi^2 = \sum_{t=1}^n M_{t,\pi}^2, \quad M_{t,\pi} = \max_{a \in \mathcal{A}} \frac{\pi(a | x_t)}{\pi_0(a | x_t)}. \quad (6)$$

Then for any objective  $i \in [m]$  and policy  $\pi \in \Pi$ , the bound  $|\hat{V}_i(\pi) - V_i(\pi)| \leq c_i(\pi)$  holds with probability at least  $1 - 2 \exp[-\beta^2/2]$ .

*Proof.* First, note that  $\hat{V}_i(\pi)$  is a weighted sum of independent  $\sigma^2$ -sub-Gaussian rewards  $Y_{t,i}$  and its mean is  $V_i(\pi)$ . Second, each reward  $Y_{t,i}$  is scaled by at most  $M_{t,\pi}$ . Therefore,  $\hat{V}_i(\pi)$  is sub-Gaussian with variance proxy  $\sigma^2 M_\pi^2 / n^2$ ; and the stated claim follows from standard concentration bounds for sub-Gaussian random variables (Boucheron et al., 2013).  $\square$

The corresponding lower confidence bound is

$$L_i(\pi) = \hat{V}_i(\pi) - c_i(\pi) \quad (7)$$

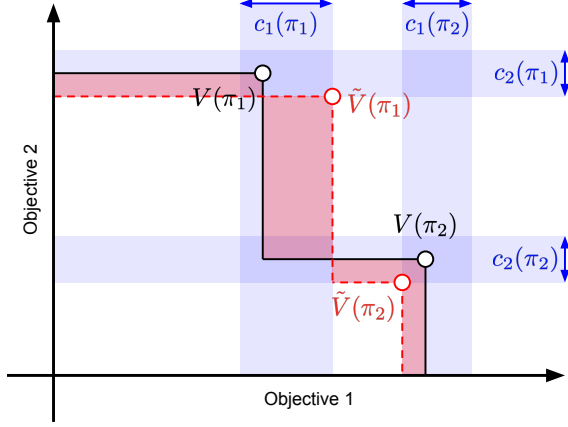


Figure 2: Illustration of Lemma 4 for  $S = \{\pi_1, \pi_2\}$ . The blue stripes represent  $\sum_{\pi \in S} \sum_{i=1}^2 c_i(\pi)$  and their areas bound the hypervolume difference (red area).

and we call it a *pessimistic IPS estimator*. When  $\beta = \sqrt{2 \log(2/\delta)}$ , the LCB holds with probability at least  $1 - \delta$  for any objective  $i \in [m]$  and policy  $\pi \in \Pi$ . We note that  $L_i(\pi)$  can be negative. Therefore, it should be clipped from below by 0 before plugging it into (3) instead of  $V_i(\pi)$ .

One notable property of  $c_i(\pi)$  is that it captures similarities of policies  $\pi$  and  $\pi_0$ . More specifically,  $c_i(\pi) = O(M_\pi)$ , where  $M_\pi$  in (6) is a sum of maximum ratios between the probabilities of taking actions under policies  $\pi$  and  $\pi_0$ . Therefore,  $c_i(\pi)$  decreases as  $\pi \rightarrow \pi_0$  and so does the uncertainty in the estimate of  $V_i(\pi)$ .

## 4 Analysis

Next we analyze the benefit of acting pessimistically. Our analysis assumes access to  $\alpha$ -approximate maximization oracles.

**Definition 1.** An oracle is  $\alpha$ -approximate if for any value function  $\tilde{V} : \Pi \rightarrow [0, 1]^m$ , it computes a set of  $K$  policies  $\tilde{S} = \text{Oracle}(\text{vol}(\cdot, \tilde{V}))$  such that

$$\text{vol}(\tilde{S}, \tilde{V}) \geq \alpha \max_{S \subseteq \Pi: |S|=K} \text{vol}(S, \tilde{V}).$$

This assumption allows us to study the statistical efficiency of our estimators without being worried about the computational cost of maximizing them. As shown later (Section 4.3), the quality of the oracle affects all our bounds identically. Thus the benefit of pessimism can be argued for any oracle and more abstract treatment is appropriate. Note that when  $\Pi$  is discrete and small, a computationally-efficient maximization oracle exists for  $\alpha = 1 - 1/e$  (Section 5.1).

This section is organized as follows. In Section 4.1, we derive error bounds for approximate maximization of

functions using their mean and pessimistic estimates. In Section 4.2, we specialize the bounds to approximate hypervolume maximization. Finally, we compare the bounds in Section 4.3. The main novelty in our analysis is that we decompose the uncertainty of hypervolume into those of its points, and show its effect on optimization. Our bounds are general, and apply beyond our IPS estimators in Section 3 and methods for optimizing them in Section 5. All omitted proofs are in Appendix A.

### 4.1 Approximate Maximization

We find it convenient to use a more abstract approach generalizing to arbitrary set functions. Let  $\Pi$  be a set of points and  $\mathcal{S} \subseteq 2^\Pi$  be a subset of its power set. Let  $g : \mathcal{S} \rightarrow \mathbb{R}$  be a set function with an approximation  $\tilde{g} : \mathcal{S} \rightarrow \mathbb{R}$ . For any set  $S \in \mathcal{S}$ , let  $c(S) \geq |g(S) - \tilde{g}(S)|$  be an upper bound on the approximation error. Let  $S_* = \arg \max_{S \in \mathcal{S}} g(S)$  be the maximizer of  $g$ . Then the  $\alpha$ -approximate maximum of  $\tilde{g}$  and the true maximum of  $g$  can be related as follows.

**Lemma 2.** Let  $\tilde{S} = \arg \max_{S \in \mathcal{S}} \tilde{g}(S)$  maximize  $\tilde{g}$  and  $\hat{S}$  be its  $\alpha$ -approximation, so that  $\tilde{g}(\hat{S}) \geq \alpha \tilde{g}(\tilde{S})$  holds for some  $\alpha \in [0, 1]$ . Then

$$g(\hat{S}) \geq \alpha g(S_*) - c(S_*) - c(\hat{S}).$$

The following bound holds for maximizing a lower bound  $L(S) = \tilde{g}(S) - c(S)$  on  $g(S)$ .

**Lemma 3.** Let  $\tilde{S} = \arg \max_{S \in \mathcal{S}} L(S)$  maximize  $L$  and  $\hat{S}$  be its  $\alpha$ -approximation, so that  $L(\hat{S}) \geq \alpha L(\tilde{S})$  holds for some  $\alpha \in [0, 1]$ . Then

$$g(\hat{S}) \geq \alpha g(S_*) - 2c(S_*).$$

Optimization of the estimated mean (Lemma 2) and the lower bound (Lemma 3) differ as follows. In the former, the error can be arbitrarily large if  $\tilde{g}$  significantly overestimates  $g$  on some set  $S$ . In the latter, the error is bounded by the error at the optimal solution  $S_*$  only. Arguably, if this one is high,  $S_*$  is hard to identify. Therefore, maximization of a lower bound yields more robust solutions.

### 4.2 Hypervolume Maximization

Now we use the error bounds in Section 4.1 to analyze IPS hypervolume maximization (Section 3.1). The key step in our argument is to relate the hypervolume under an approximation  $\tilde{V}$  to that under the true function  $V$ . We relate these through errors in individual objective estimates.

**Lemma 4.** Let  $V_i(\pi), \tilde{V}_i(\pi) \in [0, 1]$  for all  $i \in [m]$  and  $\pi \in \Pi$ . Assume that  $|V_i(\pi) - \tilde{V}_i(\pi)| \leq c_i(\pi)$  for all

$i \in [m]$  and  $\pi \in \Pi$ . Then

$$|\text{vol}(S, V) - \text{vol}(S, \hat{V})| \leq c(S) = \sum_{\pi \in S} \sum_{i=1}^m c_i(\pi).$$

The lemma says that the difference in the hypervolume of  $S$  under  $V$  and  $\hat{V}$  is bounded by the sum of differences of  $V_i$  and  $\hat{V}_i$  in individual policies  $\pi \in S$ . We visualize this in Figure 2.

To obtain an error bound for IPS hypervolume maximization, we chain Lemmas 2 and 4. Our analysis is under the assumption that (5) is clipped to  $[0, 1]$ .

**Theorem 1.** *Let  $V_i(\pi), \hat{V}_i(\pi) \in [0, 1]$  for all  $i \in [m]$  and  $\pi \in \Pi$ . Let  $|V_i(\pi) - \hat{V}_i(\pi)| \leq c_i(\pi)$  hold jointly for all  $i \in [m]$  and  $\pi \in \Pi$  with probability at least  $1 - \delta$ . Let  $\hat{S} = \text{Oracle}(\text{vol}(\cdot, \hat{V}))$  be an  $\alpha$ -approximate solution. Then with probability at least  $1 - \delta$ ,*

$$\text{vol}(\hat{S}, V) \geq \alpha \text{vol}(S_*, V) - c(S_*) - c(\hat{S}),$$

where  $c(S) = \sum_{\pi \in S} \sum_{i=1}^m c_i(\pi)$ .

*Proof.* Since  $|V_i(\pi) - \hat{V}_i(\pi)| \leq c_i(\pi)$ , by Lemma 4

$$|\text{vol}(S, V) - \text{vol}(S, \hat{V})| \leq c(S).$$

Now we apply Lemma 2, where  $g(S) = \text{vol}(S, V)$  and  $\tilde{g}(S) = \text{vol}(S, \hat{V})$ .  $\square$

Theorem 1 says that  $\text{vol}(\hat{S}, V)$  is within a multiplicative factor of  $\alpha$  of  $\text{vol}(S_*, V)$ . The additional error depends on the magnitude of confidence intervals  $c_i(\pi)$  for  $\pi \in S_* \cup \hat{S}$ . We discuss this more in Section 4.3.

Now we use the error bounds from Section 4.1 to analyze pessimistic IPS hypervolume maximization (Section 3.2). The proof is analogous to Theorem 1, with the only difference that we apply Lemma 3 instead of Lemma 2. We assume that (7) is clipped to  $[0, 1]$ .

**Theorem 2.** *Let  $L_i(\pi) = \hat{V}_i(\pi) - c_i(\pi)$  be a lower confidence bound. Let  $V_i(\pi), L_i(\pi) \in [0, 1]$  for all  $i \in [m]$  and  $\pi \in \Pi$ . Let  $|V_i(\pi) - \hat{V}_i(\pi)| \leq c_i(\pi)$  hold jointly for all  $i \in [m]$  and  $\pi \in \Pi$  with probability at least  $1 - \delta$ . Let  $\hat{S} = \text{Oracle}(\text{vol}(\cdot, L))$  be an  $\alpha$ -approximate solution. Then with probability at least  $1 - \delta$ ,*

$$\text{vol}(\hat{S}, V) \geq \alpha \text{vol}(S_*, V) - 2c(S_*),$$

where  $c(S) = \sum_{\pi \in S} \sum_{i=1}^m c_i(\pi)$ .

*Proof.* Since  $|V_i(\pi) - \hat{V}_i(\pi)| \leq c_i(\pi)$ , by Lemma 4

$$|\text{vol}(S, V) - \text{vol}(S, \hat{V})| \leq c(S).$$

Now we apply Lemma 3, where  $g(S) = \text{vol}(S, V)$  and  $\tilde{g}(S) = \text{vol}(S, L)$ .  $\square$

Theorem 2 says that  $\text{vol}(\hat{S}, V)$  is within a multiplicative factor of  $\alpha$  of  $\text{vol}(S_*, V)$ . The additional error depends on the magnitude of confidence intervals  $c_i(\pi)$  for  $\pi \in S_*$ . We discuss this more in Section 4.3.

### 4.3 Discussion

Theorems 1 and 2 are similar in two aspects. First, both say that the solution  $\hat{S}$  is  $\alpha$ -approximate up to the uncertainty in the estimate of  $V$ . Second, the uncertainty is characterized by hypervolume confidence interval widths. Specifically, when  $M_{t,\pi} = O(1)$  in (6), the widths are

$$c(S) = O(\beta \sigma K m \sqrt{1/n}).$$

As expected, they increase as the reward noise  $\sigma$  increases, the number of optimized policies  $K$  increases, the number of objectives  $m$  increases, and the probability  $1 - \delta$  with which the guarantee holds increases. The decrease with a larger sample size  $n$  is expected as well.

Theorems 1 and 2 differ only in confidence intervals. In Theorem 2, the confidence interval depends on the optimal set of policies  $S_*$  only. Therefore, when the logging policy  $\pi_0$  is near optimal,  $c(S_*)$  is small and pessimistic IPS maximization is comparable to maximizing  $\text{vol}(\cdot, V)$ , even if  $V$  is unknown and potentially poorly estimated everywhere else but around  $\pi \in S_*$ .

Such a guarantee cannot be proved for the IPS maximization in Theorem 1. To demonstrate this, suppose that there exists a policy  $\hat{\pi} \in \Pi$  such that  $\hat{V}_i(\hat{\pi}) \approx 1$  and  $c_i(\hat{\pi}) \approx 1$  for all  $i \in [m]$ . Based on  $\hat{V}_i(\hat{\pi})$  alone,  $\hat{\pi}$  is a highly-rewarding policy. However, when the confidence intervals are considered, it is clear that  $\hat{V}_i(\hat{\pi})$  are unreliable estimates. Therefore, it could be that  $V_i(\hat{\pi}) \approx 0$  for all  $i \in [m]$ . This is captured by the term  $c(\hat{S})$  in Theorem 1, which would be  $O(1)$  when  $\hat{\pi} \in \hat{S}$  and thus render the guarantee meaningless.

Finally, when the logging policy  $\pi_0$  is uniform, we do not expect any benefit of pessimism because all confidence intervals, including  $c(S_*)$  and  $c(\hat{S})$ , would have similar widths. Theorems 1 and 2 show this.

## 5 Hypervolume Optimization

Hypervolume optimization in (4) is a hard problem because both the maximization problem and hypervolume computation are. We borrow from prior works to address them. All discussions in this section apply to the value function  $V$  in (1), its IPS estimator in (5), and its pessimistic IPS estimator in (7).



### 5.1 Discrete Optimization

It is well known that  $\text{vol}(S, V)$  is monotone and submodular in  $S$  (Ulrich and Thiele, 2012). Therefore, it can be maximized greedily with guarantees as follows. In iteration  $k \in [K]$ , a policy  $\pi_k \in \Pi$  that maximally increases the hypervolume, after being added to previously selected policies  $\{\pi_\ell\}_{\ell=1}^{k-1}$ , is chosen,

$$\pi_k = \arg \max_{\pi \in \Pi} \text{vol}(\{\pi_1, \dots, \pi_{k-1}, \pi\}, V). \quad (8)$$

By Nemhauser et al. (1978), the greedy solution after  $K$  iterations  $\hat{S} = \{\pi_k\}_{k=1}^K$  is  $(1 - 1/e)$ -optimal, due to the monotonicity and submodularity of  $\text{vol}(S, V)$  in  $S$ . Unfortunately, (8) requires  $O(|\Pi|)$  hypervolume evaluations per iteration. Therefore, it is computationally inefficient when  $\Pi$  is large and cannot be applied when  $\Pi$  is continuous.

### 5.2 Policy Gradient

Rather than being limited by discrete optimization in Section 5.1, we optimize a general policy class using policy gradients (Williams, 1992; Sutton et al., 2000; Baxter and Bartlett, 2001). Let

$$\pi(a | x; \theta) = \frac{\exp[\phi(x, a)^\top \theta]}{\sum_{a' \in \mathcal{A}} \exp[\phi(x, a')^\top \theta]} \quad (9)$$

be the probability of taking action  $a \in \mathcal{A}$  in context  $x \in \mathcal{X}$  parameterized by *policy parameter*  $\theta \in \Theta$ . Here  $\phi : \mathcal{X} \times \mathcal{A} \rightarrow \mathbb{R}^d$  is an arbitrary feature mapping and  $\Theta \subseteq \mathbb{R}^d$  is the space of policy parameters.

To solve (4), we apply policy gradient to all  $K$  optimized policies. Specifically, let  $\theta_{\ell,k} \in \Theta$  be the parameter of policy  $k$  in iteration  $\ell$  and  $\theta_\ell = \bigoplus_{k=1}^K \theta_{\ell,k}$  be a concatenated parameter vector of all  $K$  policies in iteration  $\ell$ . Then, in iteration  $\ell$ , we update  $\theta_\ell$  as

$$\theta_{\ell+1} = \theta_\ell + \alpha_\ell \nabla_{\theta_\ell} \text{vol}(\{\pi(\cdot | \cdot; \theta_{\ell,k})\}_{k=1}^K, V), \quad (10)$$

where  $\alpha_\ell$  is the learning rate in iteration  $\ell$ , which can be adapted. The hypervolume is differentiable in  $\theta_\ell$  as long as  $V_i(\pi(\cdot | \cdot; \theta_{\ell,k}))$  is differentiable in  $\theta_{\ell,k}$ . This is true for any policy of form (9) plugged into the value function in (1), its IPS estimator in (5), or its pessimistic IPS estimator in (7).

In experiments, we implement (10) by automatic differentiation with Adam (Kingma and Ba, 2015). This choice was driven by the popularity of Adam and its good initial performance. We discuss other potential choices in Appendix D.

### 5.3 Hypervolume Computation

Exact computation of the hypervolume of  $K$  points is exponential in  $K$ , because it corresponds to com-

puting the union of  $K$  hyperrectangle volumes. Such computations are only feasible when  $K$  is small (Appendix E.1). Efficient exact algorithms also exist for  $m = 2$  objectives (Appendix E.2). In general, the computation can be reduced to Klee’s measure problem and the best known computational complexity is  $\tilde{O}(K^{\frac{m}{3}})$  (Chan, 2008). Despite this, many efficient approximation exists (Appendix E).

## 6 Experiments

We also evaluate the benefit of pessimism empirically. Due to space constraints, we only show representative trends and defer the rest to Appendix B.

### 6.1 Benchmarks

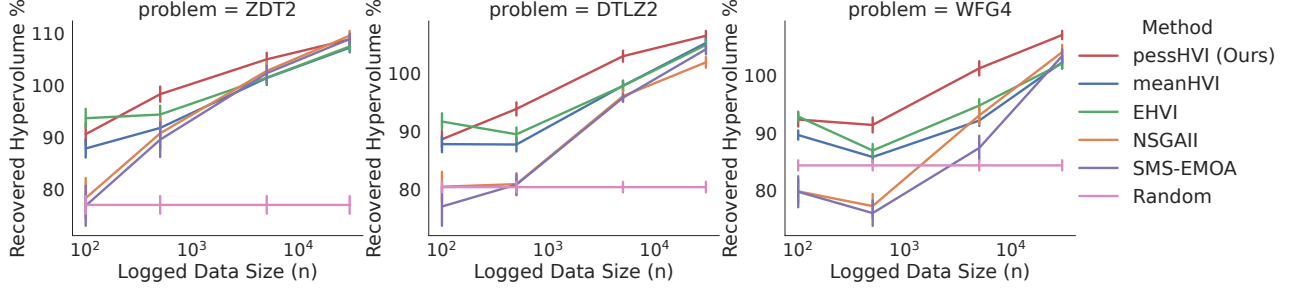
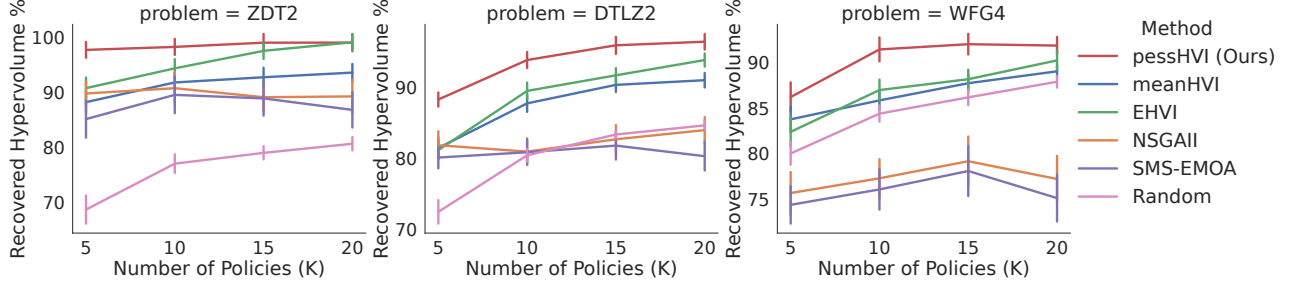
No standardized benchmarks exist for evaluating off-policy MOO. Therefore, we adapt three popular MOO benchmarks, which have been used in numerous works: ZDT (Zitzler et al., 2000), DTLZ (Deb et al., 2005), and WFG (Huband et al., 2005). ZDT is a set of bi-objective problems where the number of features can vary. Both the number of objectives and features can vary in DTLZ and WFG problems.

At a high level, we use multi-objective functions in existing benchmarks to define the mean rewards  $r(x, a)$  in (1). The mean rewards can be controlled through actions  $a$  and we optimize policies over them. Specifically, let  $\mathbb{R}^d$  be the feature space of an existing benchmark and  $f : \mathbb{R}^d \rightarrow \mathbb{R}^m$  be its multi-objective function. We split the feature space as  $\mathbb{R}^d = \mathcal{X} \times \mathcal{A}$ , where  $\mathcal{X} = \mathbb{R}^{\frac{d}{2}}$  and  $\mathcal{A} = \mathbb{R}^{\frac{d}{2}}$  are the context and action sets, respectively. The mean reward for taking action  $a \in \mathcal{A}$  in context  $x \in \mathcal{X}$  is  $r(x, a) = f(x \oplus a)$ , where  $u \oplus v$  is the concatenation of vectors  $u$  and  $v$ . We discretize  $\mathcal{A}$  by 20 random points to guarantee that the probability of taking an action in (9) can be properly normalized. The features are  $\phi(x, a) = x \oplus a \oplus \text{vec}(xa^\top) \oplus (1)$ , where  $\text{vec}(M)$  denotes the vectorization of matrix  $M$ . We introduce the cross-interaction term  $xa^\top$  to allow for context-dependent policies.

### 6.2 Evaluation Protocol

**Compared methods.** Our method is a policy gradient (Section 5.2) with the pessimistic IPS estimator in (7). We call it **pessHVI**. We set  $\beta$  in Lemma 1 to a practical value of 0.2, which performed well in our initial experiments. To show the benefit of pessimism, we compare **pessHVI** to a policy gradient with the IPS estimator in (5). We call it **meanHVI**.

We consider four additional baselines. The first baseline selects  $K$  random policies of form (9), where  $\theta$  is


 Figure 3: Comparison of **pessHVI** to baselines for  $K = 10$  while varying logged dataset size  $n$ .

 Figure 4: Comparison of **pessHVI** to baselines at  $n = 500$  while varying the number of optimized policies  $K$ .

randomly chosen from a unit ball. We call it **Random**. This baseline establishes what can be achieved with a minimal computational cost. The next two baselines are state-of-the-art genetic algorithms: NSGA-II (Deb et al., 2002) and SMS-EMOA (Beume et al., 2007). We implement them with the IPS estimator in (5).

The last baseline is a state-of-the-art approach of *expected hypervolume improvement (EHVI)* (Emmerich et al., 2005; Emmerich, 2005; Ernst et al., 2005; Yang et al., 2019). The main difficulty that we faced in implementing it was that our setting is not Bayesian, and thus there is no prior or posterior. At the end, we implement it using bootstrapping (Efron and Tibshirani, 1986), which is known to be equivalent to posterior sampling in several notable cases (Lu and Van Roy, 2017; Vaswani et al., 2018). Specifically, we take the logged dataset  $\mathcal{D}$  and resample it  $N$  times with replacement. Let  $\tilde{V}_j(\pi)$  be the IPS estimate of value function  $V(\pi)$  from resampled dataset  $j \in [N]$ . Treating it as a posterior sample, the expected hypervolume for policy  $\pi$  could be approximated as  $\frac{1}{N} \sum_{j=1}^N \text{vol}(S, \tilde{V}_j(\pi))$ . We optimize EHVI using policy gradient over the policy class in (9), exactly as in **pessHVI**.

**Hypervolume computation.** All methods are described in Appendix E. We use the exact formula in Appendix E.2 for  $m = 2$  objectives. For  $m > 2$ , we use the scalarized approximation in Appendix E.3.

**Logging policy.** We define the policy as follows. For any context  $x \in \mathcal{X}$ , let  $F_{x,a}$  indicate that  $r(x, a)$  is on

the Pareto front of  $\{r(x, a)\}_{a \in \mathcal{A}}$ . Then

$$\pi_0(a | x) \propto \varepsilon / |\mathcal{A}| + (1 - \varepsilon) F_{x,a} / \sum_{a \in \mathcal{A}} F_{x,a}. \quad (11)$$

The policy  $\pi_0$  is random with probability  $\varepsilon$  and takes near-optimal actions otherwise. We set  $\varepsilon = 0.1$ . This mimics a real-world setting where the deployed policy is already of a high quality.

**Evaluation.** We evaluate all methods by *recovered hypervolume*, which is the hypervolume of their solutions over its estimated maximum. Since all experiments are simulations, we know  $V$  and approximate the maximum hypervolume as  $\text{vol}(\tilde{S}, f)$ , where  $\tilde{S}$  are 10 000 random policies, chosen as in **Random**. The recovered hypervolume is averaged over 20 runs and we also report the standard error of its estimate. We log up to  $n = 30\,000$  points with noise  $\sigma = 1$  in each run.

### 6.3 Results

In Figures 3 and 4, we report the performance of all methods on selected ZDT, DTLZ, and WFG benchmarks with  $m = 2$  objectives and  $d = 6$  features. In Figure 3, we fix the number of optimized policies at  $K = 10$  and vary the logged dataset size  $n$ . In Figure 4, we fix the logged dataset size at  $n = 500$  and vary the number of optimized policies  $K$ . We observe two major trends. First, all methods generally improve as we increase  $n$  or  $K$ . This is expected since larger sample sizes  $n$  yield better estimates of  $V$  and larger  $K$  make hypervolume optimization easier. Sec-

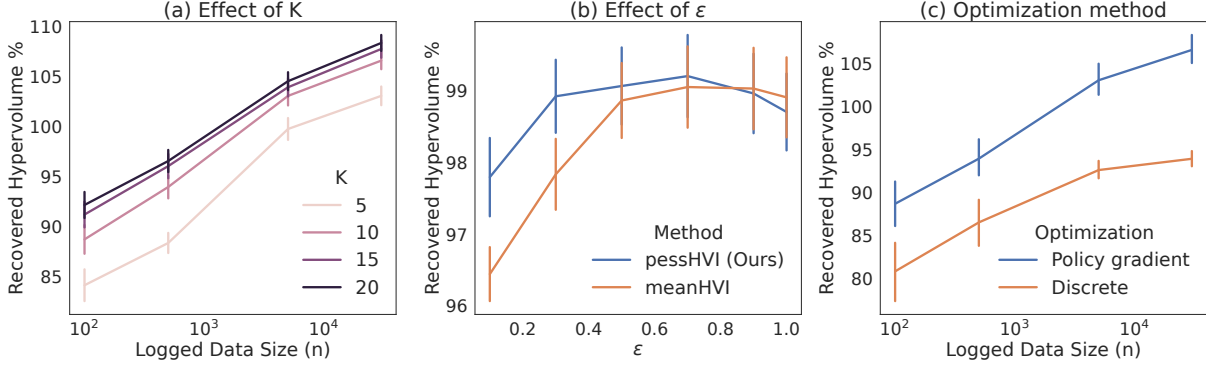


Figure 5: (a) Recovered hypervolume by **pessHVI** as a function of  $K$  and logged dataset size  $n$ . (b) The benefit of pessimism diminishes as the logging policy becomes more uniform,  $\varepsilon \rightarrow 1$ . (c) Comparison of the recovered hypervolume by policy gradient and discrete optimization in **pessHVI** with  $K = 10$ .

ond, **pessHVI** consistently outperforms **meanHVI** and all baselines. This shows that pessimistic estimators are more robust to optimization from logged data, as suggested by our analysis in Section 4.

We present additional results on 5 ZDT, 7 DTLZ, and 9 WFG problems in Appendix B; and observe similar trends to Figures 3 and 4. We also include 7 DTLZ problems with more objectives and features.

In Figure 5, we conduct an ablation study of recovered hypervolume by **pessHVI** on DTLZ2 problem. In Figure 5a, we vary the logged dataset size  $n$  and the number of optimized policies  $K$ . The recovered hypervolume improves in both. This is expected, since larger sample sizes  $n$  yield better estimates of  $V$  and larger  $K$  make hypervolume optimization easier. In Figure 5b, we vary  $\varepsilon$  in the logging policy  $\pi_0$ , and set  $n = 5000$  and  $K = 10$ . We observe that the recovered hypervolume by **pessHVI** approaches that of **meanHVI** as  $\pi_0$  becomes more uniform,  $\varepsilon \rightarrow 1$ . This confirms our theory in Section 4.3, showing that the benefit of pessimism diminishes when all confidence intervals have comparable widths. Finally, in Figure 5c, we compare policy-gradient optimization (Section 5.2) to discrete optimization over 1000 random policies (Section 5.1). The discrete optimization yields subpar results, likely due to insufficient discretization. This is why we conduct continuous optimization by policy gradients.

## 7 Related Work

Our paper is at the intersection of several fields and we review prior works in detail in Appendix F. Here we discuss only some. Our method is an instance of *a-posteriori* methods, which cover the Pareto front by a diverse set of points. Notable approaches include random scalarization in ParEGO (Knowles, 2006) and evolutionary methods, such as MOEA/D and NSGA-

II (Zhang and Li, 2007; Deb et al., 2002). The *hypervolume indicator* has become the metric of choice in several recent works that provide guarantees (Auer et al., 2016; Zhang and Golovin, 2020).

MOO has been studied extensively in the online setting, where the learning agent interactively explores the Pareto front (Drugan and Nowe, 2013). Both upper confidence bound and posterior sampling methods were proposed (Auer et al., 2016; Yahyaa and Manderick, 2015), some of which are designed for Gaussian processes (Zuluaga et al., 2013; Paria et al., 2019). Multi-objective reinforcement learning (RL) is a natural generalization of a single-step optimization and an active research area (Hayes et al., 2022).

MOO is relatively understudied in the off-policy optimization setting. Wang et al. (2022) formalized this problem as optimizing a scalarized objective, where the scalarization is learned by interacting with a policy designer. In contrast, our method is *a-posteriori*, produces a set of diverse policies without any human input, and incorporates pessimism. Two recent offline RL papers also assumed a known scalarization (Satija et al., 2021; Wu et al., 2021). Both consider a form of pessimism and apply it to finite-state models. These methods are *a-priori* because the scalarization is assumed to be known. Our method is *a-posteriori* and does not assume that the context set is finite. Finally, Zhu et al. (2023) used hypervolume to obtain expert trajectories in offline multi-objective RL. This work is empirical and does not use pessimism. In comparison, we show the value of pessimistic hypervolume optimization in both theory and experiments.

## 8 Conclusions

We study offline optimization of multi-objective policies. We propose a practical *a-posteriori* approach to



this problem, which maximizes a pessimistic hypervolume estimate for a diverse set of policies. The maximization is done by applying policy gradient jointly to all policies. We showcase the benefit of pessimism both theoretically and empirically.

This is one of the first works on offline optimization of multi-objective policies (Section 7). We analyze the benefit of pessimism generally (Section 4), beyond our IPS estimators (Section 3) and methods for optimizing them (Section 5). Consequently, our results are of a general interest, and could lay ground for analyzing other notions of diversity in a-posteriori MOO. One shortcoming of our approach is that each objective is modeled separately. Therefore, we do not take advantage of correlations among the objectives, which could improve statistical efficiency.

## References

- C. Audet, J. Bignon, D. Cartier, S. Le Digabel, and L. Salomon. Performance indicators in multiobjective optimization. *European journal of operational research*, 292(2):397–422, 2021.
- P. Auer, C.-K. Chiang, R. Ortner, and M. Drugan. Pareto front identification from stochastic bandit feedback. In *Proceedings of the 19th International Conference on Artificial Intelligence and Statistics*, 2016.
- J. Baxter and P. Bartlett. Infinite-horizon policy-gradient estimation. *Journal of Artificial Intelligence Research*, 15:319–350, 2001.
- N. Beume, B. Naujoks, and M. Emmerich. SMS-EMOA: Multiobjective selection based on dominated hypervolume. *European Journal of Operational Research*, 181(3):1653–1669, 2007.
- S. Boucheron, G. Lugosi, and P. Massart. *Concentration Inequalities: A Nonasymptotic Theory of Independence*. Oxford University Press, 2013.
- J. Branke, J. Branke, K. Deb, K. Miettinen, and R. Slowiński. *Multiobjective optimization: Interactive and evolutionary approaches*, volume 5252. Springer Science & Business Media, 2008.
- T. M. Chan. A (slightly) faster algorithm for klee’s measure problem. In *Proceedings of the twenty-fourth annual symposium on Computational geometry*, pages 94–100, 2008.
- W. Chu, L. Li, L. Reyzin, and R. Schapire. Contextual bandits with linear payoff functions. In *Proceedings of the 14th International Conference on Artificial Intelligence and Statistics*, pages 208–214, 2011.
- S. Daulton, M. Balandat, and E. Bakshy. Differentiable expected hypervolume improvement for parallel multi-objective bayesian optimization. *Advances in Neural Information Processing Systems*, 33:9851–9864, 2020.
- K. Deb, S. Agrawal, A. Pratap, and T. Meyarivan. A fast and elitist multiobjective genetic algorithm: NSGA-II. *IEEE Transactions on Evolutionary Computation*, 6(2):182–197, 2002.
- K. Deb, L. Thiele, M. Laumanns, and E. Zitzler. Scalable test problems for evolutionary multiobjective optimization. In *Evolutionary multiobjective optimization*, pages 105–145. Springer, 2005.
- T. M. Deist, S. C. Maree, T. Alderliesten, and P. A. Bosman. Multi-objective optimization by uncrowded hypervolume gradient ascent. In *Parallel Problem Solving from Nature—PPSN XVI: 16th International Conference, PPSN 2020, Leiden, The Netherlands, September 5–9, 2020, Proceedings, Part II 16*, pages 186–200. Springer, 2020.
- T. M. Deist, M. Grewal, F. J. Dankers, T. Alderliesten, and P. A. Bosman. Multi-objective learning to predict pareto fronts using hypervolume maximization. *arXiv preprint arXiv:2102.04523*, 2021.
- J.-A. Désidéri. Multiple-gradient descent algorithm (mgda) for multiobjective optimization. *Comptes Rendus Mathématique*, 350(5–6):313–318, 2012.
- M. Drugan and A. Nowe. Designing multi-objective multi-armed bandits algorithms: A study. In *Proceedings of the 2013 International Joint Conference on Neural Networks*, 2013.
- M. Dudik, D. Erhan, J. Langford, and L. Li. Doubly robust policy evaluation and optimization. *Statistical Science*, 29(4):485–511, 2014.
- B. Efron and R. Tibshirani. Bootstrap methods for standard errors, confidence intervals, and other measures of statistical accuracy. *Statistical Science*, 1(1): 54–75, 1986.
- M. Emmerich. *Single-and multi-objective evolutionary design optimization assisted by gaussian random field metamodels*. PhD thesis, Dortmund, Univ., Diss., 2005, 2005.
- M. Emmerich and A. Deutz. Time complexity and zeros of the hypervolume indicator gradient field. In *EVOLVE—a bridge between probability, set oriented numerics, and evolutionary computation III*, pages 169–193. Springer, 2014.
- M. Emmerich and A. Deutz. A tutorial on multiobjective optimization: Fundamentals and evolutionary methods. *Natural Computing*, 17:585–609, 2018.
- M. Emmerich, N. Beume, and B. Naujoks. An EMO algorithm using the hypervolume measure as selection criterion. In *Proceedings of the 3rd International Conference on Evolutionary Multi-Criterion Optimization*, pages 62–76, 2005.

- D. Ernst, P. Geurts, and L. Wehenkel. Tree-based batch mode reinforcement learning. *Journal of Machine Learning Research*, 6:503–556, 2005.
- C. F. Hayes, R. Rădulescu, E. Bargiacchi, J. Källström, M. Macfarlane, M. Reymond, T. Verstraeten, L. M. Zintgraf, R. Dazeley, F. Heintz, et al. A practical guide to multi-objective reinforcement learning and planning. *Autonomous Agents and Multi-Agent Systems*, 36(1):26, 2022.
- J. Hong, B. Kveton, M. Zaheer, S. Katariya, and M. Ghavamzadeh. Multi-task off-policy learning from bandit feedback. In *Proceedings of the 40th International Conference on Machine Learning*, 2023.
- D. G. Horvitz and D. J. Thompson. A generalization of sampling without replacement from a finite universe. *Journal of the American Statistical Association*, 47(260):663–685, 1952.
- S. Huband, L. Barone, L. While, and P. Hingston. A scalable multi-objective test problem toolkit. In *Proceedings of the 3rd International Conference on Evolutionary Multi-Criterion Optimization*, pages 280–295, 2005.
- E. Ionides. Truncated importance sampling. *Journal of Computational and Graphical Statistics*, 17(2):295–311, 2008.
- Y. Jin, Z. Yang, and Z. Wang. Is pessimism provably efficient for offline RL? In *Proceedings of the 38th International Conference on Machine Learning*, 2021.
- R. Keeney and H. Raiffa. *Decisions with Multiple Objectives: Preferences and Value Tradeoffs*. Cambridge University Press, 1993.
- D. Kingma and J. Ba. Adam: A method for stochastic optimization. In *Proceedings of the 3rd International Conference on Learning Representations*, 2015.
- J. Knowles. Parego: A hybrid algorithm with on-line landscape approximation for expensive multiobjective optimization problems. *IEEE Transactions on Evolutionary Computation*, 10(1):50–66, 2006.
- L. Li, W. Chu, J. Langford, and R. Schapire. A contextual-bandit approach to personalized news article recommendation. In *Proceedings of the 19th International Conference on World Wide Web*, 2010.
- X. Liu, X. Tong, and Q. Liu. Profiling pareto front with multi-objective stein variational gradient descent. *Advances in Neural Information Processing Systems*, 34:14721–14733, 2021.
- X. Lu and B. Van Roy. Ensemble sampling. In *Advances in Neural Information Processing Systems 30*, pages 3258–3266, 2017.
- T. Marler and J. Arora. Survey of multi-objective optimization methods for engineering. *Structural and Multidisciplinary Optimization*, 26(6):369–395, 2004.
- K. Miettinen. *Nonlinear Multiobjective Optimization*. Kluwer, 1998.
- T. Murata and H. Ishibuchi. MOGA: Multi-objective genetic algorithms. In *Proceedings of 1995 IEEE International Conference on Evolutionary Computation*, pages 289–294, 1995.
- G. L. Nemhauser, L. A. Wolsey, and M. L. Fisher. An analysis of approximations for maximizing submodular set functions - I. *Mathematical Programming*, 14(1):265–294, 1978.
- B. Paria, K. Kandasamy, and B. Póczos. A flexible framework for multi-objective Bayesian optimization using random scalarizations. In *Proceedings of the 35th Conference on Uncertainty in Artificial Intelligence*, 2019.
- A. Ponsich, A. Jaimes, and C. Coello. A survey on multiobjective evolutionary algorithms for the solution of the portfolio optimization problem and other finance and economics applications. *IEEE Transactions on Evolutionary Computation*, 17(3):321–344, 2013.
- F. P. Preparata and M. I. Shamos. *Computational geometry: an introduction*. Springer Science & Business Media, 2012.
- J. Robins, A. Rotnitzky, and L. P. Zhao. Estimation of regression coefficients when some regressors are not always observed. *Journal of the American Statistical Association*, 89(427):846–866, 1994.
- D. Roijers, L. Zintgraf, and A. Nowe. Interactive Thompson sampling for multi-objective multi-armed bandits. In *Proceedings of the 5th International Conference on Algorithmic Decision Theory*, 2017.
- H. Satija, P. S. Thomas, J. Pineau, and R. Laroché. Multi-objective SPIBB: Seldonian offline policy improvement with safety constraints in finite MDPs. In *Advances in Neural Information Processing Systems 34*, pages 2004–2017, 2021.
- O. Sener and V. Koltun. Multi-task learning as multi-objective optimization. *Advances in neural information processing systems*, 31, 2018.
- A. Strehl, J. Langford, L. Li, and S. Kakade. Learning from logged implicit exploration data. In *Advances in Neural Information Processing Systems 23*, 2010.
- R. Sutton, D. McAllester, S. Singh, and Y. Mansour. Policy gradient methods for reinforcement learning with function approximation. In *Advances in Neural Information Processing Systems 12*, pages 1057–1063, 2000.

- A. Swaminathan and T. Joachims. Counterfactual risk minimization: Learning from logged bandit feedback. In *Proceedings of the 32nd International Conference on Machine Learning*, pages 814–823, 2015a.
- A. Swaminathan and T. Joachims. The self-normalized estimator for counterfactual learning. In *Advances in Neural Information Processing Systems 28*, 2015b.
- T. Ulrich and L. Thiele. Bounding the effectiveness of hypervolume-based ( $\mu + \lambda$ )-archiving algorithms. In *International Conference on Learning and Intelligent Optimization*, pages 235–249. Springer, 2012.
- S. Vaswani, B. Kveton, Z. Wen, A. Rao, M. Schmidt, and Y. Abbasi-Yadkori. New insights into bootstrapping for bandits. *CoRR*, abs/1805.09793, 2018. URL <http://arxiv.org/abs/1805.09793>.
- H. Wang, A. Deutz, T. Bäck, and M. Emmerich. Hypervolume indicator gradient ascent multi-objective optimization. In *Evolutionary Multi-Criterion Optimization: 9th International Conference, EMO 2017, Münster, Germany, March 19-22, 2017, Proceedings 9*, pages 654–669. Springer, 2017.
- L. Wang, A. Ng, and K. Deb. *Multi-Objective Evolutionary Optimisation for Product Design and Manufacturing*. Springer, 2011.
- N. Wang, H. Wang, M. Karimzadehgan, B. Kveton, and C. Boutilier. IMO<sup>3</sup>: Interactive multi-objective off-policy optimization. In *Proceedings of the 31st International Joint Conference on Artificial Intelligence*, 2022.
- R. Williams. Simple statistical gradient-following algorithms for connectionist reinforcement learning. *Machine Learning*, 8(3-4):229–256, 1992.
- R. Wu, Y. Zhang, Z. Yang, and Z. Wang. Offline constrained multi-objective reinforcement learning via pessimistic dual value iteration. In *Advances in Neural Information Processing Systems 34*, pages 25439–25451, 2021.
- T. Xifeng, Z. Ji, and X. Peng. A multi-objective optimization model for sustainable logistics facility location. *Transportation Research Part D: Transport and Environment*, 22:45–48, 2013.
- S. Yahyaa and B. Manderick. Thompson sampling for multi-objective multi-armed bandits problem. In *Proceedings of the 23rd European Symposium on Artificial Neural Networks*, 2015.
- K. Yang, M. Emmerich, A. Deutz, and T. Bäck. Multi-objective bayesian global optimization using expected hypervolume improvement gradient. *Swarm and evolutionary computation*, 44:945–956, 2019.
- Q. Zhang and H. Li. Moea/d: A multiobjective evolutionary algorithm based on decomposition. *IEEE Transactions on evolutionary computation*, 11(6):712–731, 2007.
- R. Zhang and D. Golovin. Random hypervolume scalarizations for provable multi-objective black box optimization. In *Proceedings of the 37th International Conference on Machine Learning*, 2020.
- S. Zhou, W. Zhang, J. Jiang, W. Zhong, J. Gu, and W. Zhu. On the convergence of stochastic multi-objective gradient manipulation and beyond. *Advances in Neural Information Processing Systems*, 35:38103–38115, 2022.
- B. Zhu, M. Dang, and A. Grover. Scaling pareto-efficient decision making via offline multi-objective RL. In *Proceedings of the 11th International Conference on Learning Representations*, 2023.
- E. Zitzler, K. Deb, and L. Thiele. Comparison of multiobjective evolutionary algorithms: Empirical results. *Evolutionary computation*, 8(2):173–195, 2000.
- E. Zitzler, J. Knowles, and L. Thiele. Quality assessment of pareto set approximations. *Multiobjective optimization*, pages 373–404, 2008.
- M. Zuluaga, G. Sergeant, A. Krause, and M. Püschel. Active learning for multi-objective optimization. In *International Conference on Machine Learning*, pages 462–470. PMLR, 2013.

## A Proofs for Section 4 (Analysis)

**Lemma 2.** Let  $\tilde{S} = \arg \max_{S \in \mathcal{S}} \tilde{g}(S)$  maximize  $\tilde{g}$  and  $\hat{S}$  be its  $\alpha$ -approximation, so that  $\tilde{g}(\hat{S}) \geq \alpha \tilde{g}(\tilde{S})$  holds for some  $\alpha \in [0, 1]$ . Then

$$g(\hat{S}) \geq \alpha g(S_*) - c(S_*) - c(\hat{S}).$$

*Proof.* The claim is proved as

$$\begin{aligned} \alpha g(S_*) - g(\hat{S}) &= \alpha g(S_*) - \alpha \tilde{g}(S_*) + \alpha \tilde{g}(S_*) - g(\hat{S}) \\ &\leq \alpha(g(S_*) - \tilde{g}(S_*)) + \alpha \tilde{g}(\tilde{S}) - g(\hat{S}) \\ &\leq \alpha(g(S_*) - \tilde{g}(S_*)) + \tilde{g}(\hat{S}) - g(\hat{S}) \\ &\leq c(S_*) + c(\hat{S}). \end{aligned}$$

The first inequality holds because  $\tilde{S}$  maximizes  $\tilde{g}$ . The second inequality uses that  $\hat{S}$  is an  $\alpha$ -approximation. The last inequality follows from the definition of function  $c$  and  $\alpha \in [0, 1]$ .  $\square$

**Lemma 3.** Let  $\tilde{S} = \arg \max_{S \in \mathcal{S}} L(S)$  maximize  $L$  and  $\hat{S}$  be its  $\alpha$ -approximation, so that  $L(\hat{S}) \geq \alpha L(\tilde{S})$  holds for some  $\alpha \in [0, 1]$ . Then

$$g(\hat{S}) \geq \alpha g(S_*) - 2c(S_*).$$

*Proof.* The claim is proved as

$$\begin{aligned} \alpha g(S_*) - g(\hat{S}) &= \alpha g(S_*) - \alpha L(S_*) + \alpha L(S_*) - g(\hat{S}) \\ &\leq \alpha(g(S_*) - L(S_*)) + \alpha L(\tilde{S}) - g(\hat{S}) \\ &\leq \alpha(g(S_*) - L(S_*)) + L(\hat{S}) - g(\hat{S}) \\ &\leq 2c(S_*). \end{aligned}$$

The first inequality holds because  $\tilde{S}$  maximizes  $L$  and the second inequality uses that  $\hat{S}$  is an  $\alpha$ -approximation. The last inequality follows from  $L(S_*) = g(S_*) - c(S_*)$  and  $L(\hat{S}) - g(\hat{S}) \leq 0$ . After that, we use the definition of function  $c$  and  $\alpha \in [0, 1]$ .  $\square$

**Lemma 4.** Let  $V_i(\pi), \tilde{V}_i(\pi) \in [0, 1]$  for all  $i \in [m]$  and  $\pi \in \Pi$ . Assume that  $|V_i(\pi) - \tilde{V}_i(\pi)| \leq c_i(\pi)$  for all  $i \in [m]$  and  $\pi \in \Pi$ . Then

$$|\text{vol}(S, V) - \text{vol}(S, \tilde{V})| \leq c(S) = \sum_{\pi \in S} \sum_{i=1}^m c_i(\pi).$$

*Proof.* We start with the observation that for any two vectors  $a, b \in \{0, 1\}^d$ ,

$$\left| \prod_{i=1}^d a_i - \prod_{i=1}^d b_i \right| \leq \sum_{i=1}^d |a_i - b_i|, \quad \left| 1 - \prod_{i=1}^d (1 - a_i) - \left( 1 - \prod_{i=1}^d (1 - b_i) \right) \right| \leq \sum_{i=1}^d |a_i - b_i|. \quad (12)$$

In plain English, the difference in the logical “and” and “or” over entries of these vectors is bounded by the sum of the differences of their entries. The definition of the hypervolume together with these inequalities yields

$$\begin{aligned} |\text{vol}(S, V) - \text{vol}(S, \tilde{V})| &\leq \int_{y \in [0, 1]^m} \left| \mathbb{1} \left\{ \bigvee_{\pi \in S} \{y \leq V(\pi)\} \right\} - \mathbb{1} \left\{ \bigvee_{\pi \in S} \{y \leq \tilde{V}(\pi)\} \right\} \right| dy \\ &\leq \sum_{\pi \in S} \int_{y \in [0, 1]^m} \left| \mathbb{1} \{y \leq V(\pi)\} - \mathbb{1} \{y \leq \tilde{V}(\pi)\} \right| dy \\ &\leq \sum_{\pi \in S} \sum_{i=1}^m \int_{y \in [0, 1]} \left| \mathbb{1} \{y \leq V_i(\pi)\} - \mathbb{1} \{y \leq \tilde{V}_i(\pi)\} \right| dy \\ &= \sum_{\pi \in S} \sum_{i=1}^m |V_i(\pi) - \tilde{V}_i(\pi)| \leq \sum_{\pi \in S} \sum_{i=1}^m c_i(\pi) = c(S). \end{aligned}$$

In the first and second inequalities, we use the “or” and “and” inequalities in (12), respectively. The rest follows from basic integration identities and that we integrate over a  $[0, 1]^m$  hypercube.  $\square$

## B Additional Experiments

We conduct additional experiments on ZDT (Zitzler et al., 2000), DTLZ (Deb et al., 2005), and WFG (Huband et al., 2005) problems. The setting is the same as in Section 6.3.

### B.1 ZDT Problems

We experiment with 5 ZDT problems out of 6, with  $m = 2$  objectives and  $d = 6$  features. ZDT5 is excluded since it is a discrete optimization problem. The remaining 5 problems are continuous. Our results are reported in Figure 6. We observe that **pessHVI** consistently improves upon all baselines when  $n \geq 500$ .

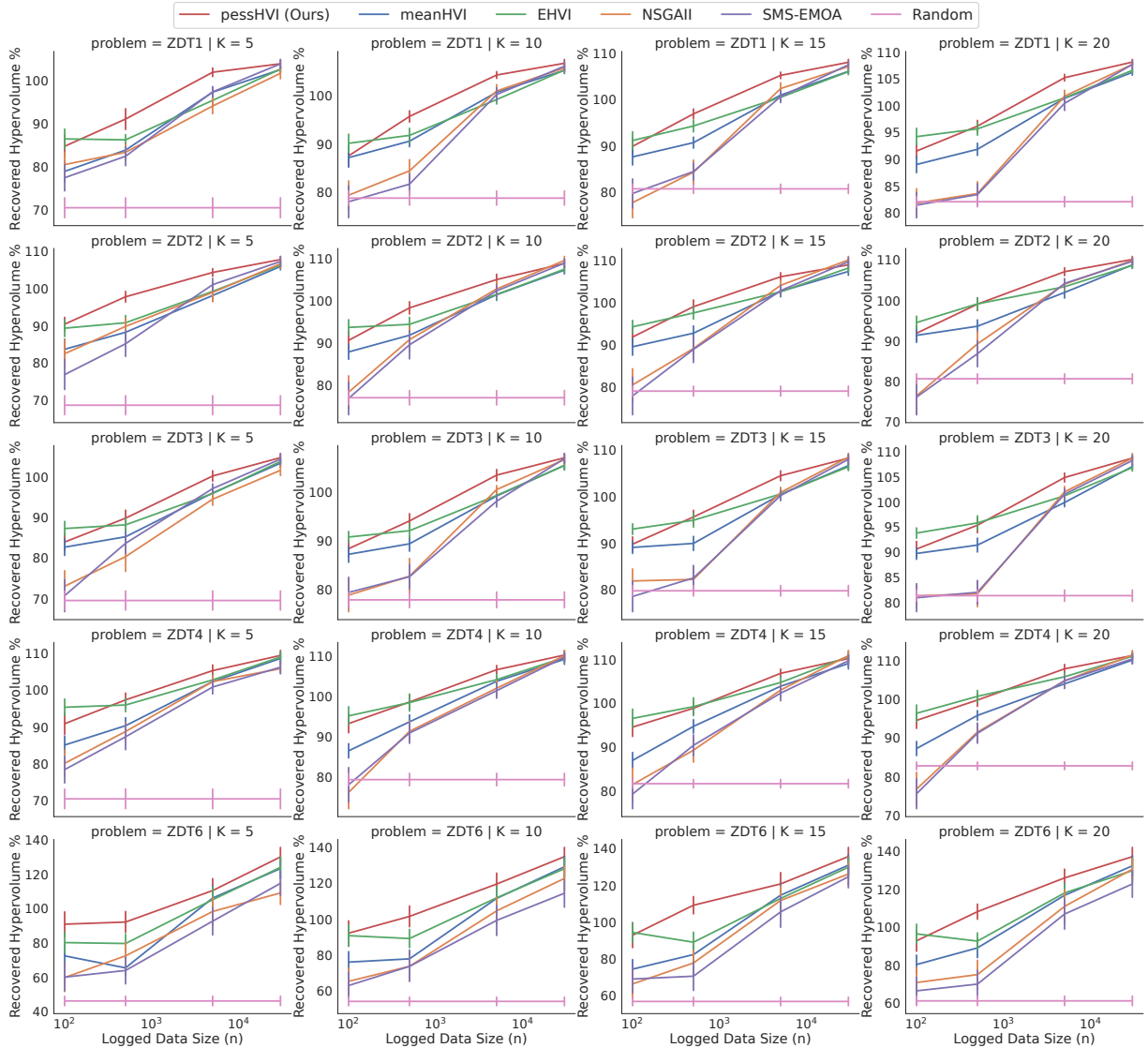


Figure 6: Evaluation of **pessHVI** and all baselines on 5 ZDT problems, for different values of  $K$  and  $n$ .

### B.2 DTLZ Problems

We experiment with 7 DTLZ problems out of 9, with  $m = 2$  objectives and  $d = 6$  features. We exclude DTLZ8 and DTLZ9 because these problems are constrained. The remaining 7 problems are unconstrained. Our results



are reported in Figure 7. We observe that **pessHVI** consistently improves upon all baselines when  $n \geq 500$ . The only exception is DTLZ6, where many methods perform well.

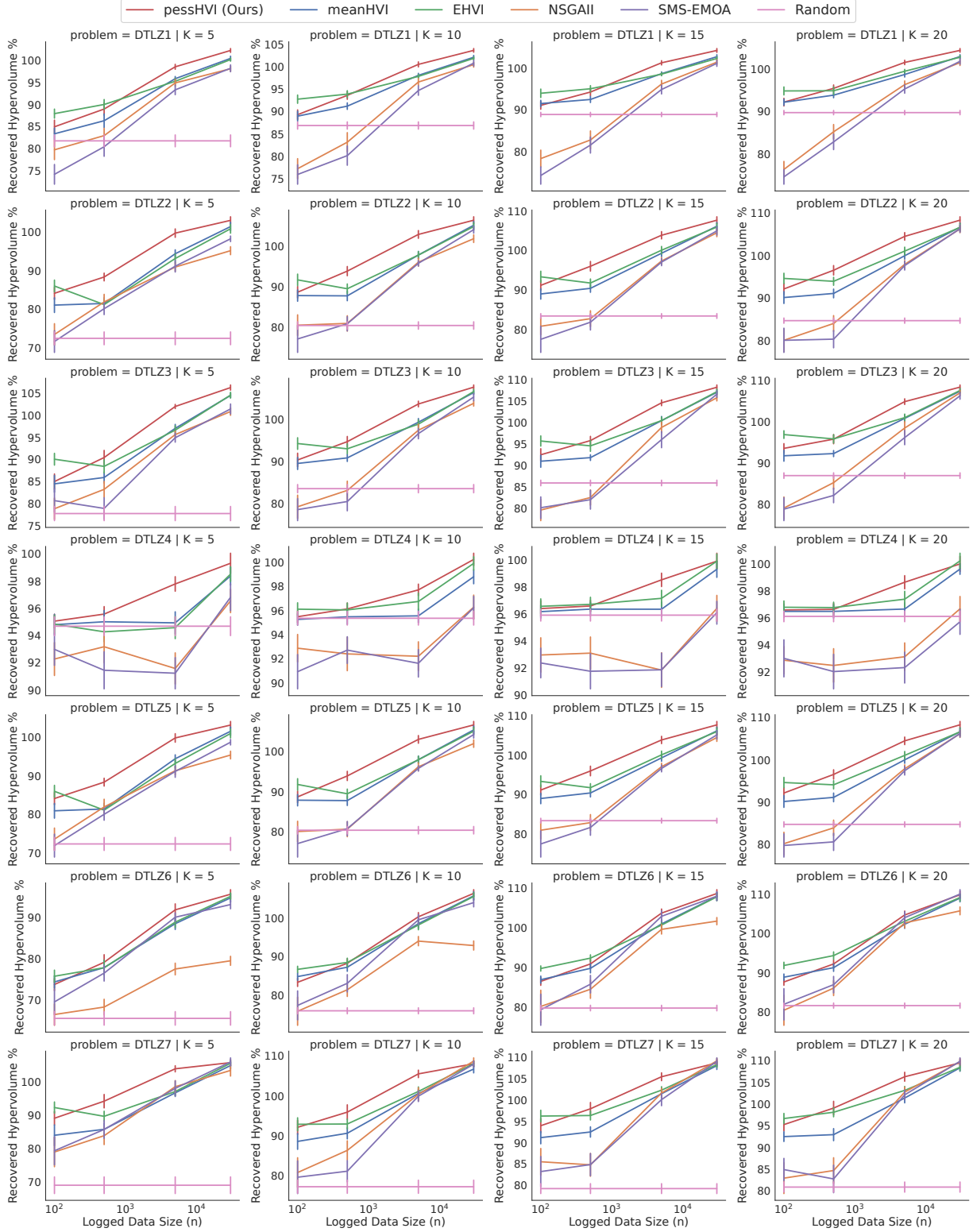


Figure 7: Evaluation of **pessHVI** and all baselines on 7 DTLZ problems, for different values of  $K$  and  $n$ .

### B.3 DTLZ Problems with 4 Objectives

Similarly to Appendix B.2, we experiment with 7 DTLZ problems, with  $m = 4$  objectives and  $d = 10$  features. The hypervolume is computed as described in Appendix E.3. Our results are reported in Figure 8. We observe that **pessHVI** consistently improves upon all baselines in 5 problems. In DTLZ4 and DTLZ6, **pessHVI** performs comparably to **meanHVI** and **EHVI**.

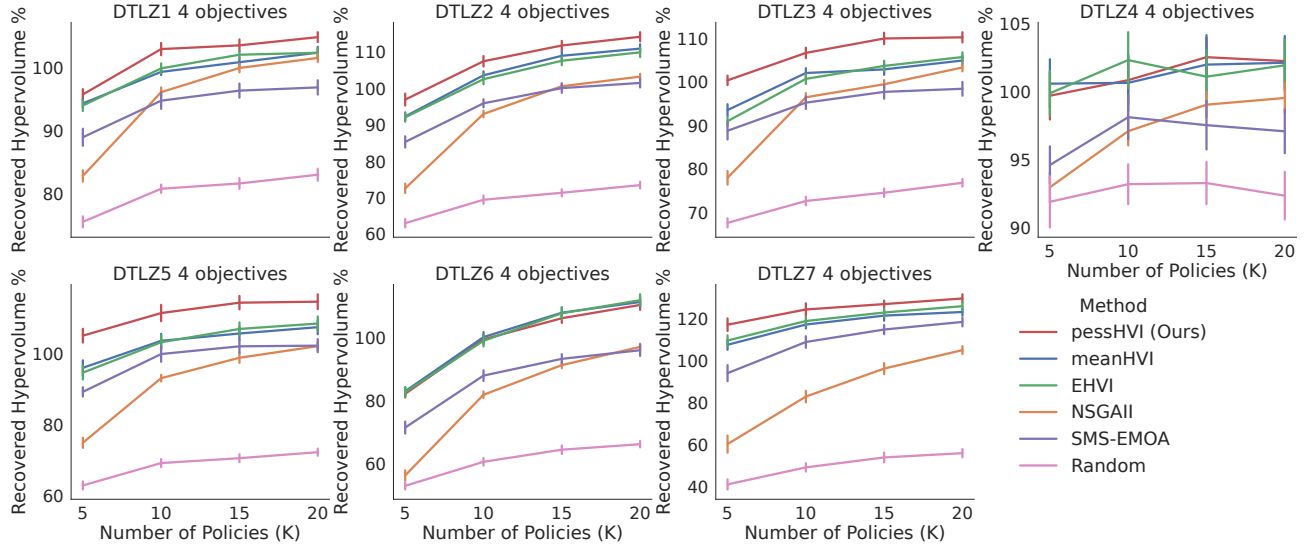


Figure 8: Evaluation of **pessHVI** and all baselines on 7 DTLZ problems with 4 objectives. We set  $n = 5000$  and vary  $K$ .

### B.4 WFG Problems

We experiment with 9 WFG problems, with  $m = 2$  objectives and  $d = 6$  features. Our results are reported in Figure 9. We observe that **pessHVI** consistently improves upon all baselines when  $n \geq 500$ . The only exception is WFG2, where many methods perform well.

## C Other Estimators

The *direct method (DM)* (Dudik et al., 2014) is a popular approach to off-policy evaluation. Using the DM, the value of policy  $\pi$  in objective  $i$  can be computed as

$$\hat{V}_i^{\text{DM}}(\pi) = \frac{1}{n} \sum_{t=1}^n \sum_{a \in \mathcal{A}} \pi(a | x_t) \hat{r}_i(x_t, a),$$

where  $\hat{r}_i(x, a)$  is the empirical mean estimate of  $r_i(x, a)$ .

The *doubly-robust method (DR)* (Robins et al., 1994; Dudik et al., 2014) combines the DM and IPS as

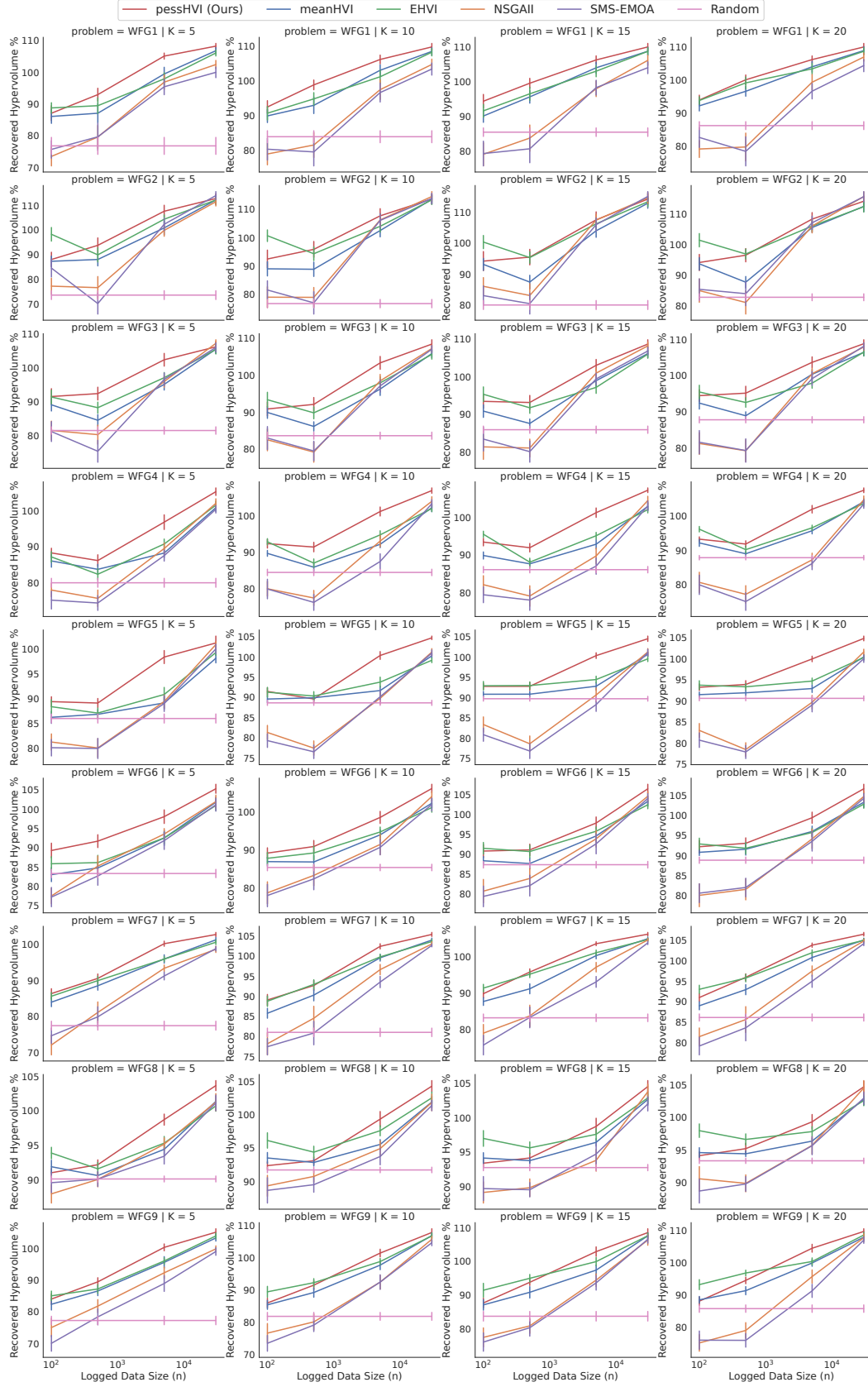
$$\hat{V}_i^{\text{DR}}(\pi) = \frac{1}{n} \sum_{t=1}^n \frac{\pi(A_t | x_t)}{\pi_0(A_t | x_t)} (Y_{t,i} - \hat{r}_i(x_t, A_t)) + \hat{V}_i^{\text{DM}}(\hat{\pi}).$$

It is popular because it combines the advantages of the DM and IPS: it is unbiased when the DM estimator is unbiased or the propensities in the IPS estimator are correctly specified.

A *self-normalized IPS (SNIPS)* estimator,

$$\hat{V}_i^{\text{SNIPS}}(\pi) = \frac{1}{\sum_{t=1}^n \frac{\pi(A_t | x_t)}{\pi_0(A_t | x_t)}} \sum_{t=1}^n \frac{\pi(A_t | x_t)}{\pi_0(A_t | x_t)} Y_{t,i},$$

is another popular approach. Unlike IPS, it is bounded but biased. However, if the logging policy is supported for all actions in each context, it is consistent (Swaminathan and Joachims, 2015b).


 Figure 9: Evaluation of **pessHVI** and all baselines on 9 WFG problems, for different values of  $K$  and  $n$ .

## D Gradient-Based Methods for Diverse Points

Gradient-based methods for finding a diverse set of points have been previously studied in the multi-task and multi-objective optimization literature. They fall into two categories:  $K$  points are optimized directly or their hypervolume is. An early approach in the former direction is algorithm MGDA of Désidéri (2012), which uses KKT conditions to compute the direction in which all objectives increase. Various extensions of MGDA have been proposed (Sener and Koltun, 2018; Zhou et al., 2022; Liu et al., 2021). These works do not directly target diversity. Gradient ascent on the hypervolume, as in our work, has been studied. One of the first works on this topic is Wang et al. (2017), who used hypervolume gradient derivations of Emmerich and Deutz (2014). The main challenge for this approach is that the hypervolume indicator is locally constant if any point is dominated. To avoid this, various modifications to steer dominated points to the boundary have been proposed (Deist et al., 2020, 2021). We believe that these methods could improve our gradient ascent optimization in Section 5.2.

## E Hypervolume Computation

We review several existing hypervolume estimators. An exact formula based on the exclusion-inclusion principle is presented in Appendix E.1. Unfortunately, it is computationally intractable when  $S$  is large. In Appendix E.2, we discuss an exact formula for two objectives that has  $O(|S| \log |S|)$  computation time. Finally, we present an approximation with  $O(|S|)$  computation time in Appendix E.3. All formulas are stated for any multi-objective function  $f : \Pi \rightarrow \mathbb{R}^m$ .

### E.1 Inclusion-Exclusion Estimator

The key insight in the inclusion-exclusion estimator (Daulton et al., 2020) is that the area of the union of two rectangles is the sum of their areas minus the area of their intersection, which is also a rectangle. In general, for hyperrectangles  $\times_{i=1}^m [a, f_i(\pi)]$ , the hypervolume can be computed as follows. Let  $2^S$  be the power set of  $S \subseteq \Pi$ . Then

$$\text{vol}(S, f) = \sum_{C \in 2^S \setminus \emptyset} (2(|C| \bmod 2) - 1) \prod_{i=1}^m \left( \min_{\pi \in C} f_i(\pi) - a \right), \quad (13)$$

where  $a \in \mathbb{R}$  represents a reference point for the beginning of the coordinate system. The computation of (13) takes  $O(2^{|S|})$  time and therefore is inefficient even for relatively small  $S$ .

### E.2 Two Objectives

For  $m = 2$  objectives, algorithms with  $O(|S| \log |S|)$  computation time exist. More specifically, let  $S = \{\pi_k\}_{k=1}^K$  and suppose that  $f_1(\pi_1) \leq \dots \leq f_1(\pi_K)$  holds, which can be done in  $O(|S| \log |S|)$  time by sorting  $\pi_k$  according to the first objective (Preparata and Shamos, 2012). Then  $f$  can be treated as a single-objective function, where  $f_1(\pi_k)$  is its input and  $f_2(\pi_k)$  is its output, and integrated along the first objective as

$$\text{vol}(S, f) = (f_1(\pi_1) - a) \left( \max_{k \in [K]} f_2(\pi_k) - a \right) + \sum_{k=1}^{K-1} (f_1(\pi_{k+1}) - f_1(\pi_k)) \left( \max_{\ell \in [K] \setminus [k]} f_2(\pi_\ell) - a \right).$$

### E.3 Random Hypervolume Scalarization

Scalarization is a mapping  $s_\lambda(f(\pi)) : \mathbb{R}^m \rightarrow \mathbb{R}$  for a given  $\lambda \in \mathbb{R}^m$ . The key idea in all scalarization methods is to reduce multiple objectives into a scalar and then optimize it. The most common scalarization techniques are linear  $s_\lambda(f(\pi)) = \sum_{i=1}^m \lambda_i f_i(\pi)$  and Chebyshev  $s_\lambda(f(\pi)) = \min_{i \in [m]} \lambda_i (f_i(\pi) - a_i)$ , where  $a \in \mathbb{R}^m$  is a reference point. Random hypervolume scalarization approximates the hypervolume indicator with random scalarizations chosen from an appropriate distribution. Specifically, Zhang and Golovin (2020) showed that the hypervolume  $\text{vol}(S, f)$  can be rewritten as

$$\text{vol}(S, f) \propto \mathbb{E}_{\lambda \sim B_m} \left[ \max_{\pi \in S} s_\lambda(f(\pi) - a) \right],$$

where  $s_\lambda(y) = \min_{i \in [m]} \max \{0, y_i / \lambda_i\}^m$ ,  $B_m$  is a unit sphere in  $\mathbb{R}^m$ , and vector  $\lambda$  is drawn uniformly from  $B_m$ . The expectation is approximated by sampling  $\lambda$ .

## F Additional Related Work

In general multi-objective optimization, the decision maker must choose a candidate  $x$  from a set of potential candidates  $\mathcal{X}$ . For each  $x \in \mathcal{X}$ , there are  $m$  objective values  $f(x) = (f_i(x))_{i=1}^m$ , where  $f_i : \mathcal{X} \rightarrow \mathbb{R}$ . Because the objectives can be traded off in many ways, many algorithms for MOO exist (Emmerich and Deutz, 2018).

In the *a-priori setting* (Branke et al., 2008), the utility of a decision maker is known in advance and used to find the optimal candidate. It is common to represent the utility function as belonging to a family of *scalarizations* of the objectives, where the objectives are weighted separately and then combined. Arguably the most popular approach is linear scalarization  $s_\lambda(f(x)) = \sum_{i=1}^m \lambda_i f_i(x)$ , where  $\lambda \in \mathbb{R}^m$  is a weight vector. In many real-world problems,  $\lambda$  is unknown in advance. In such cases, it is natural to present potential candidates to the decision maker that approximate the Pareto front well. This is known as the *a-posteriori setting* (Branke et al., 2008) and many algorithms exist for it. One popular approach is to cover the Pareto front using random scalarization (Zhang and Golovin, 2020). This was done in ParEGO (Knowles, 2006) and an evolutionary algorithm MOEAD (Zhang and Li, 2007). Other evolutionary algorithms, such as NSGA-II (Deb et al., 2002), iteratively refine a population of candidates based on various fitness metrics. Unlike our approach, none of these methods provide guarantees on the quality of the approximation and additionally do not handle uncertainty in objectives.

Regardless of the MOO method, the quality of the resulting solution needs to be measured. Intuitively, a good approximation contains a set of points that are close to the Pareto front and sufficiently diverse. Metrics that capture these two qualities are called performance indicators (Zitzler et al., 2008; Audet et al., 2021). Popular indicators are the Hausdorff distance from the approximation to the Pareto front,  $R_2$ , and hypervolume (Zitzler et al., 2000). The last has been increasingly popular and considered in several recent works (Zhang and Golovin, 2020; Auer et al., 2016). As discussed in Appendix E, hypervolume can be challenging to compute.

In the *online setting*, the decision maker interactively explores the Pareto front. Drugan and Nowe (2013) was the first work to apply bandits to MOO. They proposed a UCB1 algorithm with a scalarized objective and also a Pareto UCB1 algorithm. Auer et al. (2016) formulated the problem of the Pareto front identification as best-arm identification where at each round, a point  $x$  is chosen and a noisy observation of the objective  $f(x)$  is observed. Thompson sampling in MOO was studied in Yahyaa and Manderick (2015). A popular paradigm in MOO is to assume that the objective functions are drawn from a Gaussian process (GP) and several works have taken that approach. Zuluaga et al. (2013) is an early work with theoretical guarantees that has a similar observation model to Auer et al. (2016). Two recent works that applied GP bandits to MOO are Paria et al. (2019) and Zhang and Golovin (2020). Paria et al. (2019) minimizes the regret with respect to a known distribution of scalarization vectors. Zhang and Golovin (2020) showed that this algorithm generates a set of points that maximize random hypervolume scalarization. All above works are in the online setting, where the learning agent can interactively probe the environment to learn about objective functions. Our setting is offline.

Arguably the two closest works are Roijers et al. (2017) and Wang et al. (2022). Roijers et al. (2017) treated online MOO as a two-stage problem, where the objective functions are estimated using initial interactions with the environment and the scalarization vector is then estimated by interacting with the designer. This approach was further refined by Wang et al. (2022), who used state-of-the-art off-policy estimation techniques to estimate the objectives and analyzed their approach. The key difference in our work is that we do not put any interaction burden on the policy designer, and simply present them a diverse set of policies to choose from.